Signal Superposition Model with Mineralogy Based Spectroscopic Dielectric Model in Wireless Underground Sensor Networks

K. A. Nethravathi, and S. Ravi Shankar

Abstract—**The propagation of EM waves in soil is defined by permittivity and permeability which are in turn affected by the soil parameters such as soil moisture and texture. Therefore, a suitable Dielectric Model like MBSDM is required for the channel characterization of WUSN. Effect of soil parameters and environmental conditions on signal propagation is modelled using Superposition Model. The simulation of these stages is done in MATLAB for UG-UG, UG-AG and AG–UG scenarios. The system is further implemented on the ZYNQ ZC–702 hardware platform.**

Keywords—**Minerology Based Spectroscopic Dielectric Model, Undegroud–Underground, Underground–Aboveground, Above-ground–Underground**

I. INTRODUCTION

WIRELESS Underground Sensor Networks (WUSN) consists of a number of Under Ground (UG) sensor nodes and Above Ground (AG) data receivers; there are three different communication channels that exist in WUSNs: Underground-to-Underground (UG-UG) channel, Underground-to-Aboveground (UG-AG) channel, and aboveground-to-underground (AG-UG) channel. These channels are influenced by the changes in the soil composition, soil moisture, frequency of operation, the depth of burial of the sensor, etc.[1][2] The propagation of EM waves in soil is defined by permittivity and permeability which are in turn affected by the soil parameters such as soil moisture and texture. Therefore, a suitable Dielectric Model like MBSDM is required for the channel characterization of WUSN[3].

Path loss is used to measure the power loss in transmitting a signal through a medium. Power loss is due to absorption by the medium, reflection, refraction, interference of waves in a multipath environment etc. The propagation of waves in a medium is defined by its propagation constant, which is a combination of Attenuation constant, and Phase constant. Dielectric constant of soil is found to be dependent mainly on the Clay and Sand content, Volumetric water constant, Frequency of the signal. There are two soil dielectric models widely used, they are Semi empirical Mixing Dielectric Model (SMDM) and MBSDM[3][5][6]. The SMDM was found to deliver dielectric predictions with substantially large errors for clay silt sand soils whose dielectric data were not used for its development [3].This paper focuses on channel modeling and analysis with MBSDM.MBSDM takes into consideration the clay content, VWC and the operating frequency. Results obtained through [5] regression proves that the MBSDM parameters are influenced the most with the clay percentage of the soil samples. With increased accuracy in the values of CDC, there is a better estimation in the accuracy of the path loss values.

The authors are with the ECE DEPT, R. V. College of Engineering Bangalore, 560059, India (e-mail: nethravathika@rvce.edu.in, ravishankars@rvce.edu.in).

The paper is achieved by systematically segregating the Soil channel Model. The behaviour of the signal depends upon the electrical properties of the medium and the path traced by the signal. To model the effects of medium on the signal propagation it is necessary to develop a dielectric model which gives propagation constants through which we can estimate path loss. By knowing the path loss, quality of communication can be estimated using Monte Carlo Simulation. The effect of soil parameters and environmental conditions on signal propagation is modelled using One Ray Model and Superposition Model. A Rayleigh model is also defined to include the effects of Multipath in signal propagation.

The remainder of this paper is organized as follows: Modelling the channel is discussed in Section II. Section III discusses in detail, performance analysis of one ray and two ray algorithm. Section IV presents simulation results and inferences. The paper is finally concluded in Section V.

II. MODELLING THE CHANNEL

The channel is modelled by systematically segregating the Soil channel Model. The behavior of the signal depends upon the electrical properties of the medium and the path traced by the signal. The channel characterization mainly consists of four micro model[1].

A. Dielectric Model

To model the effects of medium on the signal propagation it is necessary to develop a dielectric model which gives propagation constants through which we can estimate path loss. MBSDM is a generalized dielectric model, where it can be applied for more number of soil types in contrast to SMDM model. This dielectric model is applicable of frequency range of 1-10GHz. It makes use of Refractive index mixing principle in which the total refractive index of the soil is calculated by weighted addition of the refractive indices of its constituents, the weights assigned is the fractional amount of each constituent in soil. The refractive index is given by equation 1 and 2.

$$n^* = n + i \cdot K \tag{1}$$

n^* - Complex Refractive index $n -$ *Refractive index*
K – Normalized attenuation coefficient

$$n_s = \begin{cases} n_d + (n_b - 1) \cdot W & , W \leq W_t \\ n_d + (n_b - 1) \cdot W_t + (n_u - 1) \cdot (W - W_t), & W \geq W_t \end{cases}$$

$$K_s = \begin{cases} K_d + K_b \cdot W & , \quad W \leq W_t \\ K_d + K_b \cdot W_t + K_u \cdot (W - W_t), & W \geq W_t \end{cases}$$

$$\tag{2}$$

$$n_d = 1.634 - 0.539 \bigg| C + 0.2748 \cdot C^2 \tag{3}$$

$$\varepsilon_{0b} = 79.8 - 85.4 \cdot C + 32.7 \cdot C^2 \ldots \tag{4}$$

$$\varepsilon' = n^2 - K^2 \tag{.5}$$

$$\varepsilon'' = 2 \cdot n \cdot K \tag{6}$$

$$K_d = 0.03952 - 0.04038 \cdot C \tag{7}$$

$$\tau_b = 1.062 \cdot 10^{-11} + 3.45 \cdot 10^{-12} \cdot C \tag{8}$$

$$W_t = 0.02863 + 0.30673 \cdot C \tag{9}$$

$$\sigma_b = 0.3112 + 0.467 \cdot C \tag{10}$$

$$\sigma_u = 0.3631 + 1.217 \cdot C \tag{.11}$$

Where n_u - Refractive index of free water , n_b - Refractive index of bounded water, n_d - Refractive index of dry soil W_t - Maximum Bound Water Fraction (MBWF) , K_d - Normalized attenuation constant of dry soil , W – Moisture content
K_b - Normalized attenuation constant of bound soil water
K_u - Normalized attenuation constant of free soil water
There is a consideration of two types of soil water, namely bound soil water (BSW) and free soil water (FSW).
The equations form 3-11 are expressed as a function of clay fraction on the assumption that clay fraction plays the dominant role among all the soil constituents. Refractive index of soil can be calculated from permittivity using equation 12 and 13.

$$n = \frac{\sqrt{\sqrt{\varepsilon'^2 + \varepsilon''^2} + \varepsilon'}}{\sqrt{2}} \tag{12}$$

$$K = \frac{\sqrt{\sqrt{\varepsilon'^2 + \varepsilon''^2} - \varepsilon'}}{\sqrt{2}} \tag{13}$$

B. Direct Wave Model

Direct wave model describes the signal propagation of Line of sight path in a medium. The path loss of DW can be calculated by using Friss transmission equation as given by equation 14 and path loss in decibels is given by equation 15.

$$\frac{P_r}{P_t} = \left[\frac{\lambda \sqrt{G_a G_b} e^{-\alpha d}}{4\pi d}\right]^2 \tag{14}$$

$$PL_{DW} \, dB = 10 \cdot \log\left(\frac{P_t}{P_r}\right)$$
$$= 6 + 20 \cdot \log(\beta) + 20 \cdot \log(d) + 8.68 \cdot \alpha \cdot d + 10 \cdot \log(G_t \cdot G_r) \tag{15}$$
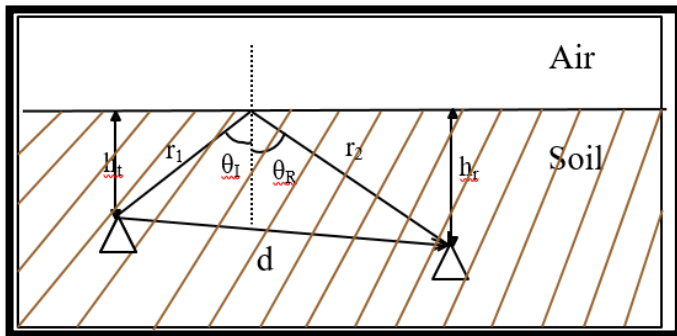

Fig 1. UG - UG Communication Scenario

P_t - Power transmitted, P_r - Power received, β - Phase constant, d – distance between transmitter and receiver G_a - Gain of transmitter antenna, G_b - Gain of receiver antenna.

C. Reflected Wave Model

Reflected wave model describes the propagation of reflected wave in the soil medium. This path incurs losses due to reflection at the soil-air interface and also travels more distance when compared to Direct Wave (DW) for same inter-node distance. The path loss equation for reflected wave is calculated in equation. (16)

$$\frac{P_r}{P_t} = \left[\frac{\lambda \cdot R \cdot \sqrt{G_c G_d} e^{-\alpha(r_1 + r_2)}}{4\pi(r_1 + r_2)}\right]^2 \tag{15}$$

Where $r_1 + r_2$ - Total distance travelled by RW in the soil medium, G_c - Gain of transmitter antenna, G_d - Gain of receiver antenna.

$$PL_{RW} = 10 \cdot \log\left(\frac{P_t}{P_r}\right)$$
$$= 6 + 20 \cdot \log(\beta) + 20 \cdot \log(r_1 + r_2) + 8.68 \cdot \alpha \cdot (r_1 + r_2) + 10 \cdot \log(G_t \cdot G_r) - 20 \log(R) \tag{16}$$

When a wave is incident at the interface of two medium a part of the wave gets reflected and a part of the wave refracted. Therefore there is loss of energy at every reflection. To account this reduction in energy, reflection coefficient is included in path loss equation. The reflection coefficient for parallel and perpendicular polarized wave is given by equations 17 and 18 respectively.

$$R_p = \frac{n_2 \cos\theta_i - n_1 \cos\theta_t}{n_2 \cos\theta_i + n_1 \cos\theta_t} \quad , \text{Parallel polarized} \tag{17}$$

$$R_s = \frac{n_1 \cos\theta_i - n_2 \cos\theta_t}{n_1 \cos\theta_i + n_2 \cos\theta_t} \quad , \text{Perpendicular Polarized} \tag{18}$$

n_1 R.I of the medium containing incident ray, θ_i - Angle of incidence, n_2 R.I of the medium containing refracted ray. θ_t - Angle of refraction.

D. Superposition Model

The line of sight signal and reflected signal superpose at the receiver and gives rise to a superposed wave. The path taken by direct wave and reflected wave are different, implies that phases of RW and DW are different; therefore they might result in constructive or destructive interference.
DW signal at receiver is given by equation 19.

$$r_{DW}(t) = Re\left\{\frac{\lambda}{4\pi}\left[\frac{\sqrt{G_a G_b} e^{-\gamma d}}{d} \; u(t)\right] e^{j2\pi ft}\right\} \tag{19}$$

RW signal at receiver is given by equation 20.

$$r_{RW}(t) = Re\left\{\frac{\lambda}{4\pi}\left[\frac{R * \sqrt{G_c G_d} e^{-\gamma(r_1 + r_2)}}{r_1 + r_2} \; u(t)\right] e^{j2\pi ft}\right\} \tag{20}$$

The phases of RW and DW signals are different. Therefore SW signal at receiver is calculated as shown in the equation 21.

$$r_{SW}(t) = Re\left\{\frac{\lambda}{4\pi}\left[\frac{\sqrt{G_a G_b} e^{-\gamma d}}{d} u(t) + \frac{R \sqrt{G_c G_d} e^{-\gamma(r_1 + r_2)}}{r_1 + r_2} u(t - \tau)\right] e^{j2\pi ft}\right\} \tag{.,.....21}$$

where $r_{DW}(t)$ - DW signal at receiver , $r_{RW}(t)$ - RW signal at receiver, $r_{SW}(t)$ - SW signal at receiver $u(t)$ - Transmitted signal, R – Reflection coefficient .If spreading of signal from transmitter is less and time delay between DW and SW is less than coherent time, then $u(t) \approx u(t - \tau)$. Substituting $u(t) \approx u(t - \tau)$ in equation 21 and common terms separated. Thereby equation 21 is modified as shown in the equation 22.

$$r_{SW}(t) = Re\left\{\frac{\lambda}{4\pi}\frac{\sqrt{G_a G_b} e^{-\gamma d}}{d} u(t)\left[1 + \frac{R \sqrt{G_c G_d} \; e^{-\gamma(r_1 + r_2)} \; d \; e^{\gamma d}}{\sqrt{G_a G_b} \; (r_1 + r_2)}\right] e^{j2\pi ft}\right\} \tag{22}$$

By substituting $\Delta r = (r_1 + r_2) - d$, $\Delta\phi = \beta((r_1 + r_2) - d)$, $\Delta\phi = \beta * \Delta r$ in equation 22, equation 23 is formed.

$$r_{SW}(t) = Re\{\frac{\lambda}{4\pi}\frac{\sqrt{G_aG_b}e^{-\gamma d}}{d} u(t)\left[1 + \frac{R\sqrt{G_cG_d}\ e^{-\gamma\ \Delta r}\ d}{\sqrt{G_aG_b}\ (r_1+r_2)}\right]e^{j2\pi ft}\} \quad \dots (23)$$

From equation 23, Path loss is calculated as shown in equation

$$\frac{P_t}{P_r} = \left[\frac{\lambda\sqrt{G_aG_b}e^{-\alpha d}}{4\pi d}\right]^{-2}\left|1 + \frac{R\sqrt{G_cG_d}\ e^{-\gamma\ \Delta r}\ d}{\sqrt{G_aG_b}\ (r_1+r_2)}\right|^{-2} \quad (24)$$

$$R = \Gamma\ e^{j\theta} \quad (25)$$

θ- Phase of reflection coefficient

$$z = \left|1 + \frac{R\sqrt{G_cG_d}\ e^{-\gamma\ \Delta r}\ d}{\sqrt{G_aG_b}\ (r_1+r_2)}\right|^2 \quad (25)$$

Substituting equation 23 in equation 24, equation 25 is formed.

$$z = \left|1 + \frac{\Gamma\ e^{j\theta}\ \sqrt{G_cG_d}\ e^{-\alpha\ \Delta r}\ e^{-\beta\ \Delta r}\ d}{\sqrt{G_aG_b}\ (r_1+r_2)}\right|^2 \quad (25)$$

Equation 25 is modified as shown in equation 26.

$$z = \left|1 + \frac{\Gamma\ \sqrt{G_cG_d}\ e^{-\alpha\ \Delta r}\ e^{j\ (\theta-\Delta\phi)}\ d}{\sqrt{G_aG_b}\ (r_1+r_2)}\right|^2 \dots \quad (26)$$

$\Delta\phi = \beta((r_1 + r_2) - d)$, Let $A = \frac{\Gamma\ \sqrt{G_cG_d}\ e^{-\alpha\ \Delta r}\ d}{\sqrt{G_aG_b}\ (r_1+r_2)}$ $\Delta r = (r_1 + r_2) - d$

Substituting equation 26 equation 27 is formed.

$$z = \left|1 + A\ e^{j\ (\theta-\Delta\phi)}\ \right|^2 \quad (27)$$

$$\frac{P_t}{P_r} = \left[\frac{\lambda\sqrt{G_aG_b}e^{-\alpha d}}{4\pi d}\right]^{-2}|z|^{-2} \quad (28)$$

Path loss can be expressed in dBm as given in equation 29.

$$PL_{SW} = 10 \cdot \log_{10}(\frac{P_t}{P_r}) = PL_{DW} - 10 \cdot \log_{10}(z) \quad (29)$$

Fig. 2. Signal superposition model

III.   PERFORMANCE ANALYSIS OF CHANNEL MODEL

To analyze the performance of the communication through any medium a complete view of the characteristics of the same, play a vital role. In the case of underground communication, major soil parameters to be considered are volumetric water content (VWC), fraction of clay, silt and sand; the deployment aspects such as the burial depth of the sensor nodes and the distance between them and the operating frequency. With the above mentioned parameters the complex dielectric constant (CDC) of the soil is computed. Since the soil is considered to be non-magnetic in nature, the standard value of permeability is assumed. The attenuation and the phase constant for the given soil are calculated using the Dielectric constant and Loss Factor obtained from MBSDM model. The propagation constant so calculated gives the actual measure of the total loss along the direct path during signal transmission and hence know the amount of signal strength at the receiving end. By knowing the

received signal strength BER can be simulated using Monte Carlo simulation as follows:

Algorithm for One-ray model

i.   Generate a stream of input bits.
ii. Generate random variable using inverse of Gaussian Probability Density Function.
iii. Calculate noise voltage by multiplying Gaussian random variable with Standard Deviation of noise.
iv. Estimate Rayleigh variable using Quantile function of Rayleigh Distribution.
v.   Calculate the received signal considering the effect of Rayleigh fading coefficient and noise voltage.
vi. By using suitable detection condition, determine BER.

Algorithm for Two-ray model

i.   Generate a stream of input bits whose magnitude is evaluated with the aid of Superposition Model.
ii. Generate an array of random variable of length 1×2 (for DW and RW) using inverse of Gaussian Probability Density Function.
iii. Calculate an array of noise voltage of length 1×2 (for DW and RW) by multiplying Gaussian random variable with Standard Deviation of noise.
iv. Estimate Rayleigh variable of same size using Quantile function of Rayleigh Distribution.
v.   Calculate the received signal considering the effect of Rayleigh fading coefficient and noise voltage. By using suitable detection condition, determine BER.

IV.   RESULT ANALYSIS AND INFERENCES

The signal is transmitted through the channel with operating frequencies ranging from 1-10 G Hz, moisture content ranging from 5-25 %, inter node distance from 0-8 m , depth varying from 0-2 m.To study the behavior of permittivity of soil with operating frequency , Clay fraction and VWC, the parameters were set as shown in Table I.

TABLE I
SIMULATION PARAMETERS FOR DC, LF VS FREQUENCY

Parameters	Values
Frequency	1-10G Hz
Temperature	20-25 °C
Clay (%)	10 – 60
Moisture (VWC in %)	{3.2, 8, 8.8, 13.2, 18.4, 29.1, 29.7, 38.2, 39.4}

From fig 3 and fig 4 it can be observed that DC of soil decreases with increase in frequency, where as LF increases with frequency. Both DC and LF are found to be increasing along with increase in VWC. Therefore it is better to operate at lower frequency as it incurs less attenuation loss.
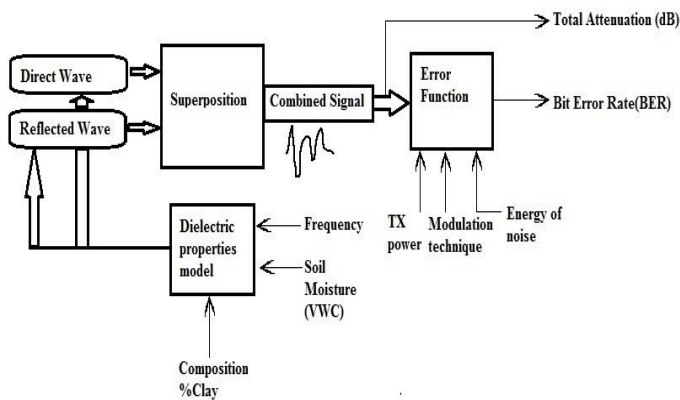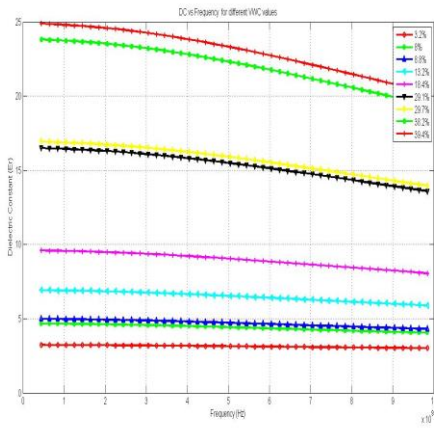
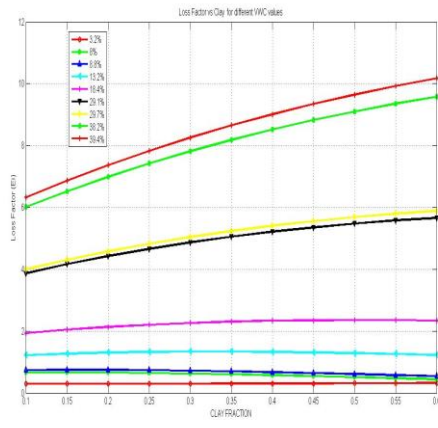Fig 3. DC vs frequency for different VWC

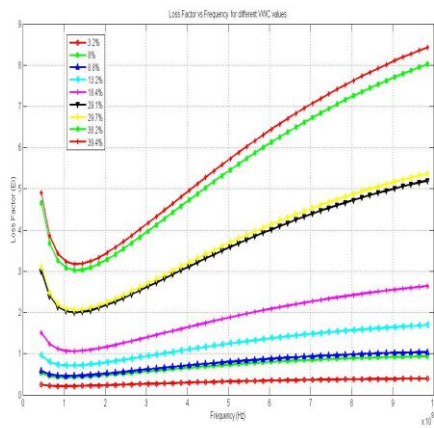Fig. 5. Variation of DC and LF with Clay fraction for different VWC values

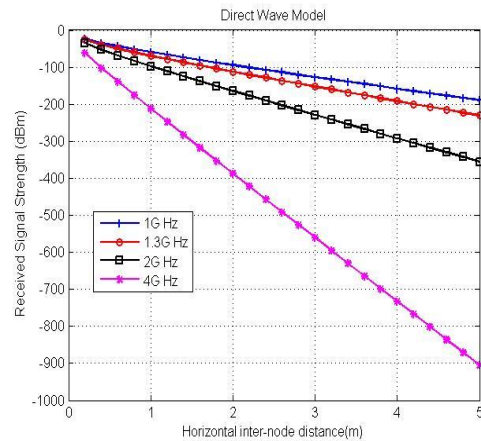Fig 4. LF vs frequency for different VWC

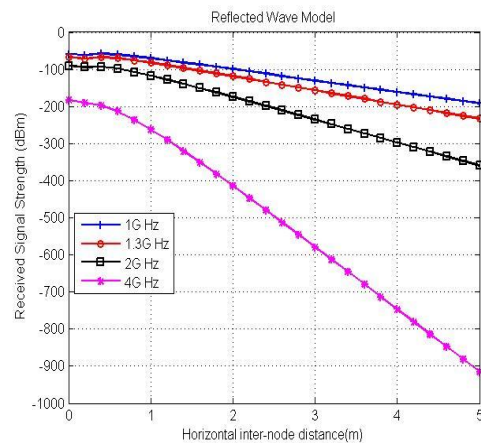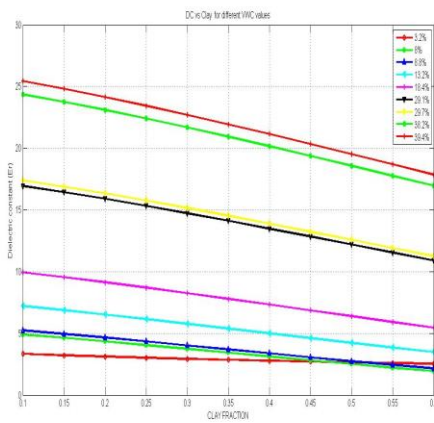Fig. 6. RSS versus Horizontal inter node distance for DW

Fig. 7. RSS versus horizontal inter-node distance for RW

As the clay fraction increases the capacity of the soil to hold water increases thus making soil lossier in nature. This phenomenon can be observed in fig 5. It can be concluded that for soil with higher clay content attenuation is high

The variation of RSS with respect to the location of nodes. The distance between the nodes is varied from 0-5 m for a transmit power of 10 dBm. The same analysis is repeated for operating frequencies of 1, 1.3,2,4 G Hz.
From fig 6, it can be concluded that as horizontal inter-node distance increases, the RSS decreases. RSS decreases drastically

for higher operating frequencies. Therefore, operating frequency should be optimum for better communication.
It can be noticed from the fig 7 that The RSS of Reflected Wave Model decreases with increasing horizontal inter-node distance apart from decreasing drastically for higher distances.

For the same horizontal inter-node distance, reflected wave suffers more path loss in comparison to direct wave. The comparison of path loss of the DW and RW for 4GHz frequency is shown in the table II.

TABLE II
COMPARISON OF PATH LOSS OF DW AND RW

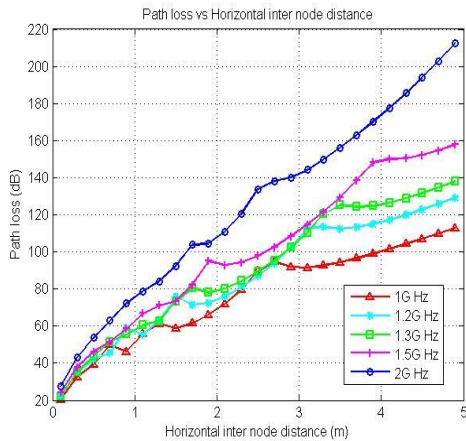| Inter-node distance (m)	DW path loss (dBm)	RW path loss (dBm)
1	-200	-270
2	-395	-410
3	-565	-595

Fig 8. Path Loss versus horizontal inter-node distance for SW.

It can be observed from fig 8 that Path Loss of the SW increases with increasing horizontal inter-node distance. The Path Loss of SW increases drastically for higher frequencies.
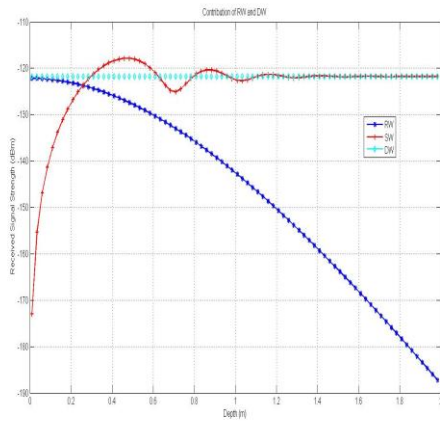The fluctuations in the path loss is due to the interference of DW and RW.

Fig 9. RSS versus Depth for DW, RW, SW

Fig 9 depicts the contribution of Direct and Reflected Waves for the Superposed Wave. It is clear from that Effect of Reflected wave decreases with increase in depth Therefore Superposed Wave (SW) has fluctuations at lower depths Superposed wave follows the Direct Wave for higher depths i.e. Direct Wave dominates over Reflected Wave at higher depths.

From the fig 10 and fig 11 it can be inferred that Path Loss of Superposed Wave Model is fluctuating at lower depths and this fluctuation decreases with increase in the depth. This fluctuation at lower depths is because of constructive and

destructive interference of Direct and Reflected Wave. The contribution of Reflected Wave is negligible at higher depths, hence there are no fluctuations at higher depths i.e. Direct Wave dominates over Reflected Wave at higher depths.[7]
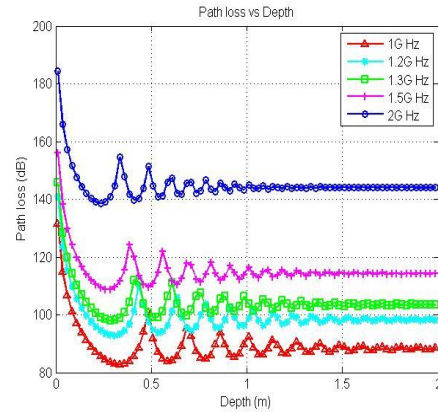

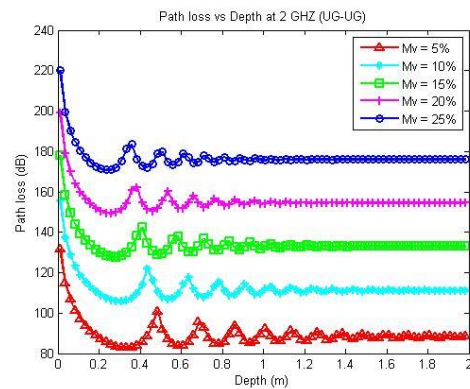Fig 10. Path Loss versus depth for different frequencies

Fig 11. Path Loss versus depth for different Path Loss versus depth for different VWC

Path loss increases with increase in frequency and VWC as attenuation constant increases with them. Variation of BER for Non-Rayleigh and Rayleigh Model is depicted in fig 12 and fig 13 . BER increases with increase in horizontal inter-node distance. BER for Rayleigh Model is more compared to Non-Raleigh Model for same inter-node distance. By increasing transmitted power, the quality of communication increases.
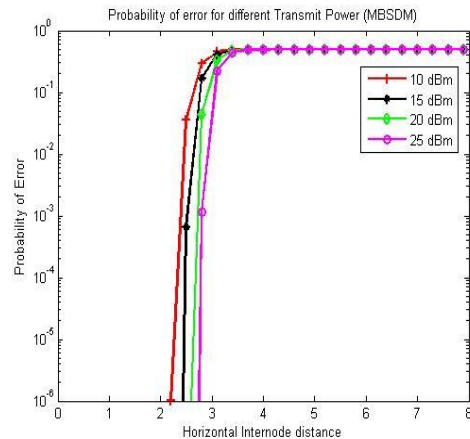

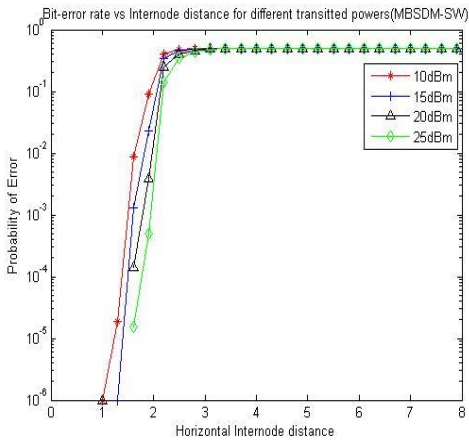Fig 12. BER versus horizontal inter-node distance for Non- Rayleigh Model

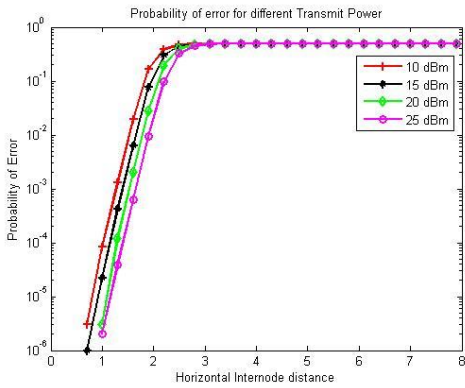Fig 13. BER versus horizontal inter-node distance for Rayleigh Model

Fig. 14. BER versus Horizontal inter-node distance for Direct Wave

Fig 14 and 15 make us aware about the contribution of RW to the SW. This can be analyzed by parametric analysis of BER using monte carlo simulation for DW and SW. The BER results are compared for DW and SW for different horizontal inter-node distances at transmitted power of 10 dBm in the table III.

TABLE III
COMPARISON OF BER OF DW AND SW

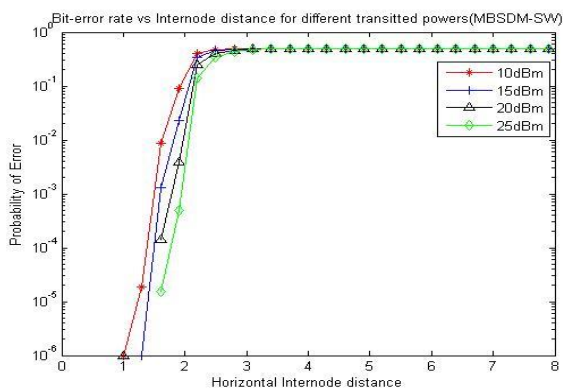| Inter-node distance (m)	DW – BER	SW – BER
0.5	1e-6	0
0.7	3e-6	0
1	1e-4	1e-6
1.3	1e-3	2e-5
1.6	0.02	0.01

Fig. 15. BER versus Horizontal inter-node distance for Superposed Wave

From fig 14 and fig 15, it can be concluded that Both Superposed Wave Model and Direct Wave Model have increasing BER with increase in horizontal inter-node distance. Superposed Wave Model has less BER compared to Direct Wave Model for same horizontal inter-node distance. The contribution of reflected signal facilitates communication over larger distances.

From the fig 16, The BER simulation is done for operating frequency of 1GHz, 4-PAM and 16-QAM Modulation technique. Dielectric constant and loss factor of soil varies with moisture content. The effect of which can be noticed in path loss. It can be inferred from the fig 17 that BER increases with VWC as Loss factor increases with moisture content.

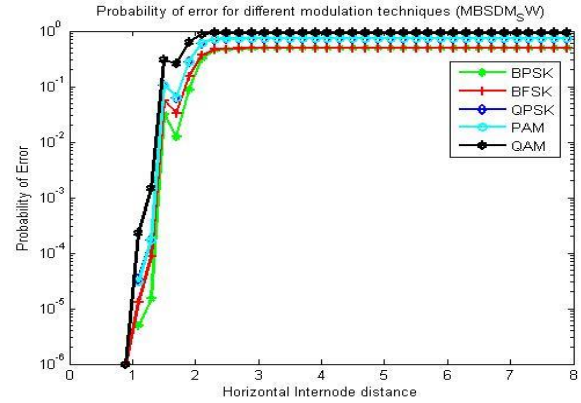The table V tabulates the values of BER given in fig 17.

Fig. 16. BER versus horizontal inter-node distance for Different Modulation Techniques

TABLE IV
BER FOR DIFFERENT MODULATION SCHEMES

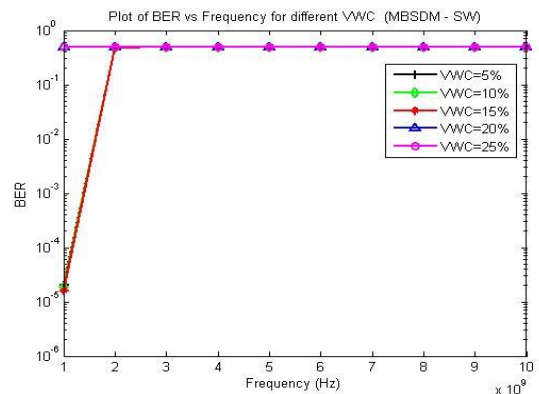| Modulation	BPSK	BFSK	QPSK	PAM	QAM
Distance (M)					
0.7	0	0	0	0	0
0.9	0	1e-4	0	0	1.000e-06
1.1	0.5e-5	0.13e-4	3.4e-05	3.00e-05	2.270e-04
1.3	1.5e-5	0.0001	0.0002	1.74e-04	0.0014
1.5	0.0322	0.0552	0.1069	0.1075	0.3038
1.7	0.0124	0.0323	0.0627	0.06390	0.2548
3.9	0.5006		0.7501	0.75	0.9375

Fig. 17. BER versus operating frequency for Different VWC values

TABLE V
BER FOR DIFFERENT VWC

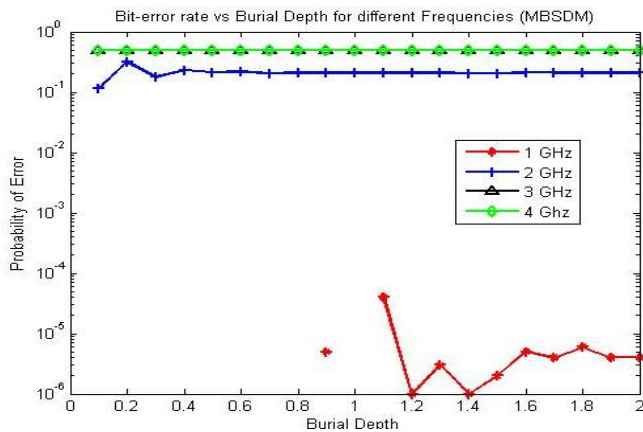| VWC Frq (G Hz)	5 %		10 %	15 %	20 %	25 %
1	2.00 e-5		1.9 e-5	1.60e-5	0.4944	0.4992
2			0.4804	0.4805	0.5000	0.5001
3	0.4821		0.4996	0.4994	0.4998	0.5011
4	0.5012		0.5005	0.4997	0.4992	0.5003
5	0.4995		0.5002	0.4996	0.4998	0.4993
6	0.5005		0.5007	0.4994	0.5006	0.4999
7	0.5000		0.4996	0.4996	0.5002	0.4997
8	0.4996		0.4997	0.4999	0.5001	0.5009
9	0.4996		0.5001	0.4994	0.4994	0.4994
10	0.5000 0.4999		0.5002	0.4997	0.5001	0.5012

Fig. 18. BER versus burial depth for different frequencies

It can be concluded from fig 18 that BER increases drastically with frequency owing to increase in Loss Factor. The fluctuation in BER stabilizes after a certain depth due to decrease in contribution of RW.

A. Implementation on ZynQ Development Board

BER depends not only upon Path loss but also on type of Modulation scheme employed. For communication there always exists a trade-off between quality of communication and data rate that can be serviced. To deliver service based upon the requirement the analysis of BER with distance for different modulation scheme is necessary.

TABLE VI
BER OBTAINED FROM ZYNQ BOARD

Modulation Distance(M)	BPSK	BFSK	QPSK	PAM	QAM
1.15	62e-6	75e-6	95e-6	90e-6	1e-6
1.25	65e-6	80e-6	0.135e-6	0.128e-6	0.2e-3
1.35	0.17e-3	0.35e-6	0.46e-3	0.43e-6	0.009
1.9	0.075	0.1333	0.1456	0.135	0.2
2.0	0.176	0.240	0.322	0.256	0.38

The analysis of the same is depicted in figure 16 and is tabulated in Table IV Monte Carlo simulation for Rayleigh Channel for SW is done on ZynQ development Board. The ZynQ board yielded similar results as that of simulation which is tabulated in table VI.

The BER for same inter-node distance is found to be increasing in the order BPSK, BFSK, 4-PAM, QPSK and 16-QAM modulation.

V. CONCLUSION

The characterization of the channel for WUSNs is done for the UG-UG, AG-UG and UG-AG links using MBSDM model owing to the fact that it is more generalized. to predict the signal strength at the receiving end more accurately, Superposed Wave model is proposed, which considers the effect of both DW and RW. The channel model for SW is tested for different transmit powers by measuring the RSS for inter-node distance. Plot of BER reveals that BER decreases from 1e-4 to 1e-6 with transmit power increasing from 10 to 25 dBm, from this it is clear that better quality of communication can be achieved by stepping up transmitted power. The results obtained from ZynQ board shows similar trend in BER.

REFERENCES

[1] Agnelo R. Silva, "Channel Characterization for Wireless Underground Sensor Networks", Ph.D thesis, University of Nebraska – Lincoln, April 2010.

[2] Ian F. Akyildiz, Mehmet C. Vuran Valery, Li Li, "Characteristics of Underground Channel for Wireless Underground Sensor Networks", Sixth Annual Mediterranean Ad Hoc Networking Workshop, Corfu, Greece, June 2007 pp. 92-99.

[3] V. L. Mironov, L. G. Kosolapova, and S. V. Fomin, "Soil Dielectric Model Accounting for Contribution of Bound Water Spectra through Clay Content", Vol.4, No.1, 2008 pp. 31-35, PIERS Online.

[4] Hu Xiaoya, Gao Chao, Wang Bingwen, Xiong Wei " Channel modeling for wireless underground sensor networks", *35th IEEE Annual Computer Software and Applications Conference 2011,* pp.248-254.

[5] Valery Mironov and Pavel Babrov, "Spectroscopic Microwave dielectric model of moist soils", Advances in Geoscience and Remote Sensing, pp. 279-302, http://www.intechopen.com.

[6] V. L. Mironov, L. G. Kosolapova, and S. V. Fomin, "Physically and Mineralogically Based Spectroscopic Dielectric Model for Moist Soils", *IEEEE Transactions on Geoscience and Remote Sensing*, Vol.47, No. 7, July 2009 pp. 2059-2070.

[7] Xiaoqing Yu, PuteWu et al., "electromagnetic wave propagation in soil for wireless underground sensor networks", *Progress In Electromagnetics Research M,* Vol. 30, pp. 112-133, 2013.

[8] Neil R. Peplinski et al., "Dielectric Properties of Soils in the 0.3-1.3-GHz Range", *IEEE transactions on Geoscience and Remote sensing,* vol. 33, no. 3,pp. 803-807, May 1995.

[9] W.G.Fano et al., "Dielectric Properties of Soils", *Annual Report Conference on Electrical Insulation and Dielectric Phenomena*, pp. 75-78 , 2001.

[10] Valery L. Mironov et al., "Generalized Refractive Mixing Dielectric Model for Moist soils", *IEEE transactions on Geoscience and Remote sensing,* vol. 42, no. 4, pp. 773-785, April 2004.

[11] V.L. Mironov "Spectral Dielectric Properties of Moist Soils in the Microwave Band", *IEEE Trans. Geoscience and Remote sensing,* vol. 22, no. 2, pp. 3474-3477, 2004.

[12] James R. Wang et al., "An Empirical Model for the Complex Dielectric Permittivity of Soils as a Function of Water Content", Laboratory for Atmospheric Sciences, NASA/Goddard Space Flight Centre, Greenbelt, Feb 1990.